V International Conference on Particle-based Methods – Fundamentals and Applications
PARTICLES 2017
P. Wriggers, M. Bischoff, E. Oñate, D.R.J. Owen, & T. Zohdi (Eds)

DISCRETE ELEMENT MODELLING OF GRANULAR COLUMN COLLAPSE TESTS WITH INDUSTRIAL APPLICATIONS

JOEL TORRES-SERRA[1], DEEPAK R. TUNUGUNTLA[2], IRANA F.C. DENISSEN[2], ANTONIO RODRÍGUEZ-FERRAN[3] AND ENRIQUE ROMERO[3]

[1] Técnicas Mecánicas Ilerdenses, S.L.
Polígono industrial Camí dels Frares, c. Alcarràs, parc. 66, 25190 Lleida, Spain
e-mail: j.torres@tmipal.com

[2] Multi-Scale Mechanics, Engineering Technology/MESA+
University of Twente, P.O. Box 217, 7500 AE Enschede, The Netherlands

[3] Universitat Politècnica de Catalunya – BarcelonaTech
Campus Nord, c. Jordi Girona, 1-3, 08034 Barcelona, Spain

Key words: DEM, granular column collapse, particle size distribution, coarse-graining.

Abstract. The effect of particle size distribution on dry granular flows of spherical particles has been numerically investigated. A quasi-two-dimensional granular column collapse set-up has been modelled using the Discrete Element Method (DEM). Systems formed by monodisperse particles of radius $R = 0.01$ m and polydisperse particles of the same average radius and coefficient of uniformity $C_u = 1.9$ have been studied for initial granular columns aspect ratios of 1.1 and 2.2. The results using monodisperse and narrow particle size distributions show similar evolution of the run-out profiles, the final run-out distance being reached in less than one second in every configuration. Averaged velocity fields have been obtained, from which peak values of longitudinal and vertical components of velocity have been found.

1 INTRODUCTION

Describing the behaviour of granular materials is a challenging issue for the packaging industry where bulk handling equipment is designed to handle a wide range of powders and bulk solids varying in both physical and mechanical properties. As a result, not only performance of packaging equipment is negatively affected but also are packaging quality and the whole process itself. Furthermore, environmental conditions such as relative humidity also have serious consequences on the efficiency of material conveying techniques.

Thereby even a small improvement in the efficiency of equipment can lead to both significant financial and environmental benefits.

For this purpose, the granular column collapse set-up is used, as it is known to provide deep insights into the dynamics of granular flow regimes both at particle and bulk level [1]. However, as an alternative to experiments, in this paper the discrete element method (DEM) is utilised because of its ability to effectively control and quantify the micro-scale parameters, what is often very difficult to do in an experiment. Several particle properties, including size [2], shape [3] and density [4], are known to affect the bulk macroscopic behaviour. However, as a stepping stone, this study focusses on numerically investigating the effects of varying particle size distribution by utilising the open-source particle simulation package MercuryDPM [5]. Eventually, the goal is to systematically model the effects of varying particle properties, which in turn would help us define and improve decision-making strategies for the design of packaging equipment.

The following sections present the simulation methodology and the findings of our investigation.

2 METHODOLOGY

2.1 DEM model

In the implemented simulations, a linear normal contact model is used to describe particle motion of the translational degrees of freedom, where the inter-particle contact parameters comprise normal stiffness, k_n, and viscous dissipation, γ_n, as well as the tangential counterparts k_t, γ_t. Additionally, the tangential or sliding friction coefficient, μ_t, is used to define a Coulomb-type coupling between the tangential and normal components of the force acting on particle i, $\mathbf{f}_i$, due to contact with neighbour particles j:

$$\mathbf{f}_i = \sum_j \left(f_n \mathbf{n} + f_t \mathbf{t}\right) \tag{1a}$$

$$f_n = \begin{cases} 0 & \delta_n \leq 0 \\ k_n \delta_n + \gamma_n v_n & \delta_n > 0 \end{cases} \tag{1b}$$

$$f_t = \min\left\{\mu_t f_n; k_t \delta_t + \gamma_t v_t\right\} \tag{1c}$$

where δ_n is overlap between particles, δ_t is tangential spring of active contacts and v_n, v_t are the normal and tangential components of relative velocity, respectively. Regarding rotational degrees of freedom, the contribution to torque of inter-particle rolling resistance is accounted for using stiffness, dissipation and friction coefficients, k_r, γ_r, μ_r, and torsional resistance is described using parameters k_o, γ_o, μ_o, which, along with tangential coefficients, define total torque on particle i, $\mathbf{q}_i$, as discussed by Luding [6]:

$$\mathbf{q}_i = \sum_j \left[\left(\mathbf{l}_i \times \mathbf{f}_i\right) + \mathbf{q}_i^t + \mathbf{q}_i^r + \mathbf{q}_i^o\right] \tag{2}$$

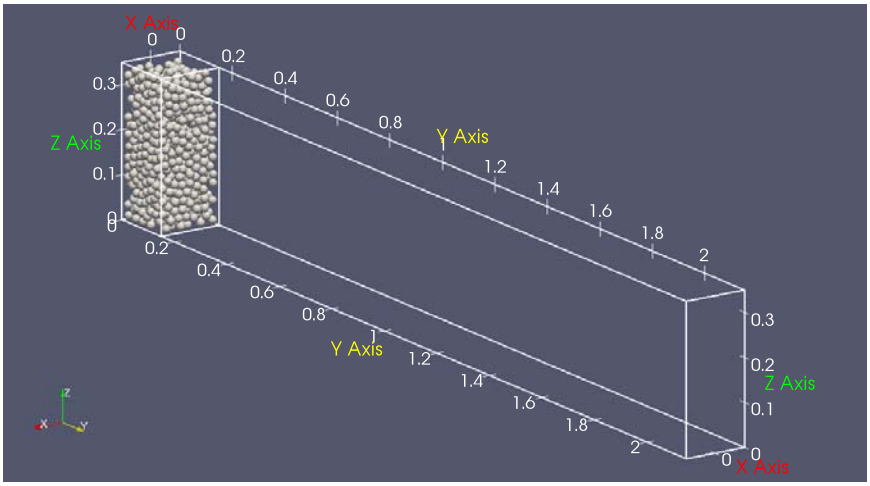

Figure 1: Simulation set-up of the granular column collapse channel. Dimensions in [m]

where $\mathbf{l}_i$ is the branch vector and $\mathbf{q}_i^t$, $\mathbf{q}_i^t$, $\mathbf{q}_i^t$ are respectively the tangential, rolling and torsional components of total torque.

2.2 Granular column collapse set-up

A quasi-two-dimensional granular column collapse simulation set-up has been studied to assess the influence of particle size polydispersity on the run-out process. The considered domain consists in a prismatic horizontal channel of total length 2150 mm, height 350 mm and width 150 mm, along which run-out takes place. An auxiliary vertical wall is initially placed at length 150 mm, which forms a reservoir of square section where the granular columns are generated, as shown in Figure 1. Granular piles are allowed to settle in the reservoir under gravity, until stationary initial packing conditions are reached. The arrangement of particles is then instantaneously released onto the channel, by removing the auxiliary vertical wall from the simulation domain.

Spherical particles have been simulated, with particle density $\rho_p = 2000\ \mathrm{kg\,m^{-3}}$. Two different particle size distributions (PSD) of the granular material have been studied:

- Monodisperse PSD with particle radius $R = 0.01$ m;
- Polydisperse PSD with average particle radius $R = 0.01$ m. Randomly generated radii are obtained by linear interpolation between input values from $R = 5.0 \times 10^{-3}$ m to $R = 1.5 \times 10^{-2}$ m, as shown in Figure 2. The coefficient of uniformity of the polydisperse particle system is $C_u := D_{60}/D_{10} = 1.9$.

Moreover, simulations with two different number of particles of the system have been carried out, being $N = \{500, 1000\}$ for assemblies of monodisperse spheres and respectively adjusted to $N = \{405, 809\}$ in the polydisperse case, by enforcing the total mass of the system to be preserved.

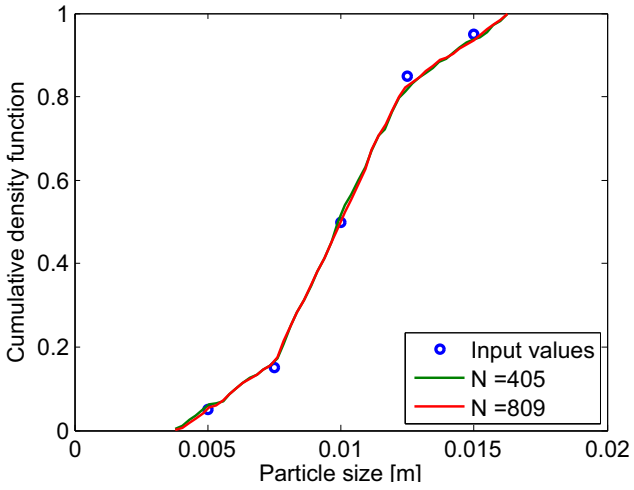

Figure 2: Cumulative distribution function for the polydisperse PSD

Table 1: Inter-particle contact parameters of granular column collapse simulations

		Stiffness $[\mathrm{N\,m^{-1}}]$ $k_\square$	Dissipation $[\mathrm{N\,s\,m^{-1}}]$ $\gamma_\square$	Friction coefficient $\mu_\square$
Normal	$\square_n$	2.0×10^4	0.5	—
Tangential	$\square_t$	2.0×10^3	0.1	0.5
Rolling	$\square_r$	2.0×10^3	0.1	0.05
Torsional	$\square_o$	2.0×10^3	0.1	0.05

Mechanical properties of the contacts are shown in Table 1. Since a linear spring–dashpot contact model has been used, overdamping of the system is prevented by controlling the value of contact eigenfrequencies. The values of normal stiffness and viscous dissipation of the particles fulfil the following relation:

$$\gamma_n = \sqrt{2 k_n m_{\min}} \tag{3}$$

where $m_{\min}$ corresponds to the minimum particle mass of the system. Mechanical parameters governing particle–wall interactions have not been modified with respect to inter-particle contact properties.

3 RESULTS AND DISCUSSION

Total mass of the system is $m = 4.189$ kg and $m = 4.245$ kg respectively for the case with $N = 500$ monodisperse particles and $N = 405$ polydisperse particles. Analogously, total mass is $m = 8.378$ kg and $m = 8.4806$ kg respectively for the case with $N = 1000$ monodisperse particles and $N = 809$ polydisperse particles. Therefore, the considered particle system configurations are approximately equivalent with respect to the total mass of the system.

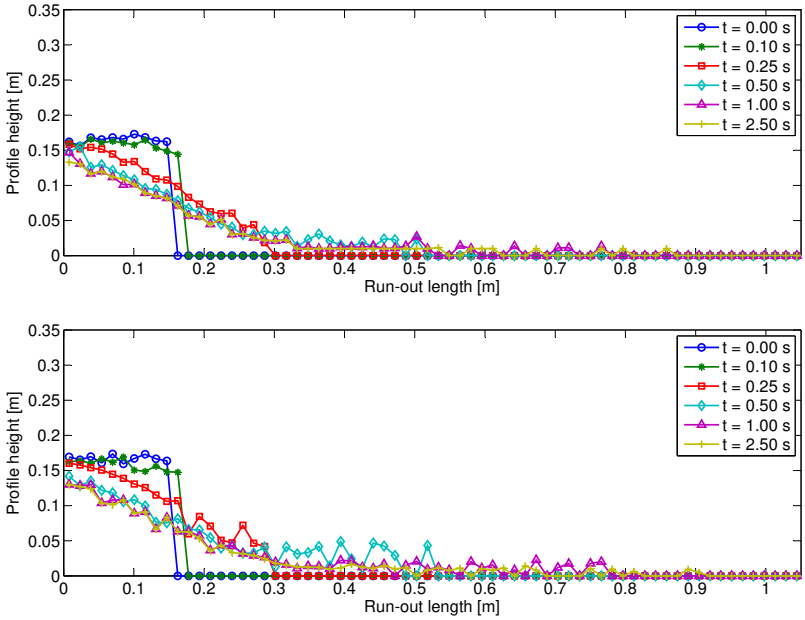

Figure 3: Lateral profile tracking from $t = 0$ s to $t = 2.5$ s: $N = 500$ monodisperse particles (upper); and $N = 405$ polydisperse particles (lower)

System stability is controlled by adjusting the normal contact parameters, which results in a critical contact time, t_c, and coefficient of restitution, r, that are $t_c = 1.438 \times 10^{-3}$ and $r = 0.918$ for the monodisperse case, and $t_c = 3.325 \times 10^{-4}$ and $r = 0.686$ for the case with size polydispersity. Introducing size polydispersity while preserving average particle size by mass leads to smaller stable time increments in the numerical scheme. Additionally, the critical restitution coefficient is decreased, although to a lesser extent, in the polydisperse case.

Evolution of flow profiles has been tracked in the YZ plane, time being measured from the onset of flow, in order to identify final run-out distance at the end of the simulation. Initial column heights are $H = 0.165$ m and $H = 0.167$ m respectively for the case with $N = 500$ monodisperse particles and $N = 405$ polydisperse particles, resulting in a column aspect ratio $a = 1.1$, with respect to the reservoir base length (0.150 m). At the same time, column heights are $H = 0.336$ m and $H = 0.326$ m respectively for the case with $N = 1000$ monodisperse particles and $N = 809$ polydisperse particles, the initial column aspect ratio being $a = 2.2$. Particle positions are averaged over the channel width, along which granular flow is mainly homogeneous, thus providing the lateral observation of the run-out, as shown in Figure 3 and Figure 4. It is observed that the whole collapse to run-out process lasts for about a second in every configuration. Thereafter, the system is found to remain in a stable configuration with a constant morphology of the free surface and a few moving particles located near the flow front. Final run-out distance is therefore defined as the channel length comprising 95% of the mass of the system, considering 5% ot the

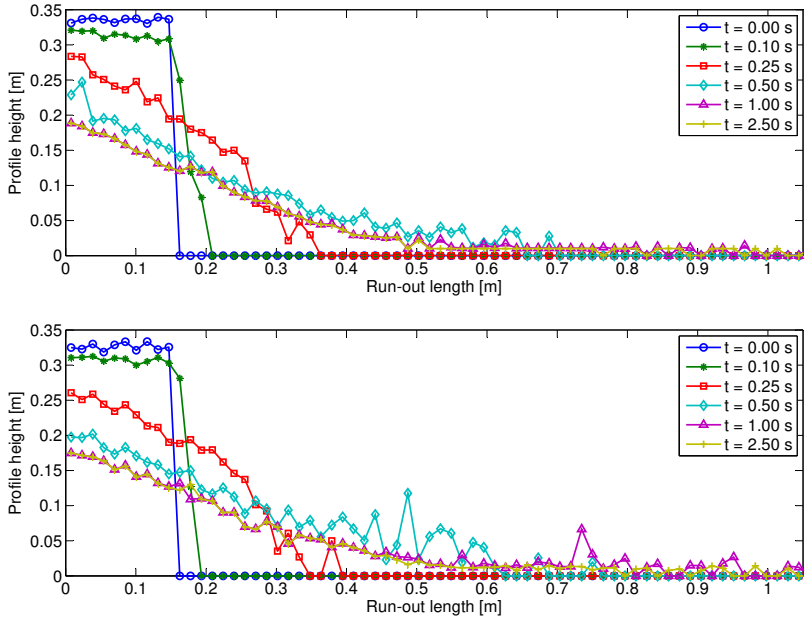

Figure 4: Lateral profile tracking from $t = 0$ s to $t = 2.5$ s: $N = 1000$ monodisperse particles (upper); and $N = 809$ polydisperse particles (lower)

total mass corresponds to particles ahead of the flow front. After run-out, at $t = 1$ s, final run-out distance for the configurations with $N = 500$ monodisperse particles and $N = 405$ polydisperse particles are $L = 0.387$ m and $L = 0.418$ m, respectively. In addition, for the computations with $N = 1000$ monodisperse particles and $N = 809$ polydisperse particles, final run-out distances are respectively $L = 0.572$ m and $L = 0.603$ m.

In order to map the particle data onto a continuum field, an accurate micro-macro mapping technique called coarse graining is used [7, 8]. Coarse-grained velocity field, fully averaged over the channel width (X Axis), $\langle \mathbf{v}(\mathbf{x},t)\rangle_x$, is obtained by:

$$\langle \mathbf{v}(\mathbf{x},t)\rangle_x = \frac{\left\langle \sum_{i=1}^{N} m_i \mathbf{v}_i(t)\phi(\mathbf{x}-\mathbf{x}_i(t))\right\rangle_x}{\left\langle \sum_{i=1}^{N} m_i \phi(\mathbf{x}-\mathbf{x}_i(t))\right\rangle_x} \tag{4}$$

where m_i is the particle mass, $\mathbf{v}_i(t)$ is the time-dependent particle velocity and $\phi(\mathbf{x}-\mathbf{x}_i(t))$ is a coarse-graining function. In this study, a gaussian function has been used, with scale equal to the maximum particle radius of the particle assembly, $w = \max_i\{R_i\}$. Table 2 summarizes peak values for longitudinal, v_y, and vertical, v_z —negative downwards, components of velocity during run-out.

As far as the simulations with $N = 500$ and $N = 405$ particles are concerned, peak v_y is larger for the case with polydisperse spheres. Maximum values attained are in agreement in the case of $N = 1000$ and $N = 809$ particles, althoguh peak v_z is observed at a later time during run-out for the case of size polydisperse particles. Figure 5 shows maps of

Table 2: Peak values of v_y and v_z at respective time instants, t

	v_y $[\mathrm{m\,s^{-1}}]$	t [s]	v_z $[\mathrm{m\,s^{-1}}]$	t [s]
Monodisperse $N = 500$	0.855	0.25	−0.769	0.20
Polydisperse $N = 405$	1.078	0.30	−0.757	0.25
Monodisperse $N = 1000$	1.517	0.35	−1.413	0.30
Polydisperse $N = 809$	1.588	0.55	−1.154	0.30

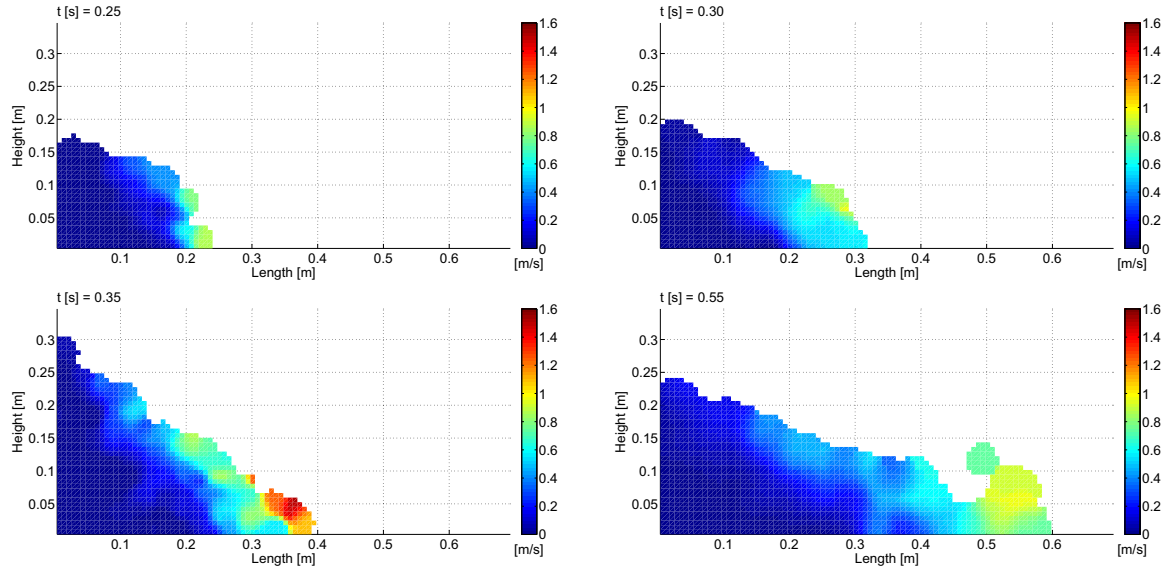

Figure 5: Peak v_y velocity maps: $N = 500$ monodisperse particles (upper-left); $N = 405$ polydisperse particles (upper-right); $N = 1000$ monodisperse particles (lower-left); $N = 809$ polydisperse particles (lower-right)

v_y along the channel (Y Axis) at the respective times when peak velocity is reached. Vertical component of velocity (Z Axis), at respective time instants of peak values of v_z, is shown in Figure 6.

In light of the results, notable differences in flow behaviour have not been identified when comparing granular collapse of spheres of radius $R = 0.01$ with another sphere assembly of the same average particle size and corresponding to a narrow-graded material. Evolution of laterial profiles during run-out is analogous, resulting in final deposits in the form of shallow slopes. The velocity fields established during flow propagation also show similar trends, as for all simulations a flow front is rapidly developed, dominated by the longitudinal component of velocity.

4 CONCLUDING REMARKS

The effect of particle size on run-out profiles, final run-out distances and averaged peak velocities has been analysed for two granular column collapse set-ups using two

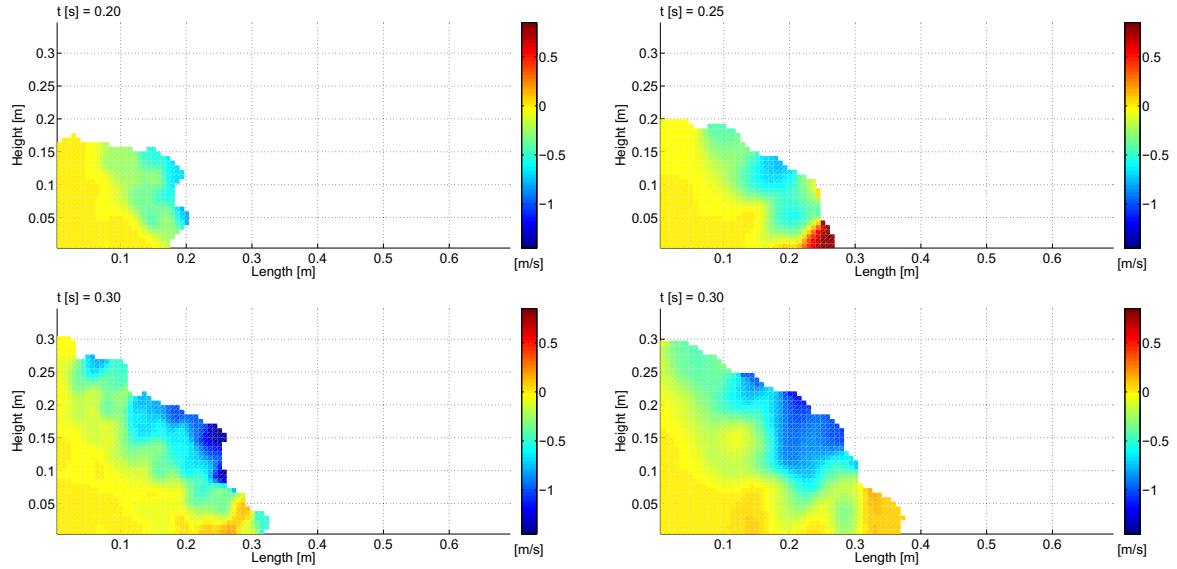

Figure 6: Peak v_z velocity maps: $N = 500$ monodisperse particles (upper-left); $N = 405$ polydisperse particles (upper-right); $N = 1000$ monodisperse particles (lower-left); $N = 809$ polydisperse particles (lower-right)

monodisperse and polydisperse spherical particles. In future investigations, the influence of other particle properties and environmental effects are to be studied, including:

- Average partice size reduction, leading to an increase of the number of particles and different flow behaviours,
- Polydispersity in particle shape, comparing the use of spherical and non-spherical particles, namely ellipsoids, and
- Hygroscopicity effect, adding water content to particle assemblies to observe capillary behaviour in the pendular state.

ACKNOWLEDGEMENTS

The first author would like to acknowledge the financial support provided by Project 2014 DI 075, "Optimization of dosing systems for bulk solids using experimental and numerical techniques", funded by the Industrial Doctorates Plan of the Government of Catalonia.

REFERENCES

[1] Torres-Serra, J., Romero, E., Rodríguez-Ferran, A., Caba, J., Arderiu, X., Padullés, J.-M. and González, J. Flowability of granular materials with industrial applications. An experimental approach. In: *Powders and Grains 2017: 8th International Con-*

ference on Micromechanics of Granular Media EPJ Web of Conferences, Vol. 140, (2017).

[2] Lu, H., Guo, X., Liu, Y. and Gong, X. Effect of Particle Size on Flow Mode and Flow Characteristics of Pulverized Coal. *KONA Powder Part. J.* (2015) **32**:143–153.

[3] Fu, X., Huck, D., Makein, L., Armstrong, B., Willen, U. and Freeman, T. Effect of particle shape and size on flow properties of lactose powders. *Particuology* (2012) **10**(2):203–208.

[4] Tunuguntla, D., Bokhove, O. and Thornton, A. A mixture theory for size and density segregation in shallow granular free-surface flows. *J. Fluid Mech.* (2014) **749**:99–112.

[5] Weinhart, T., Tunuguntla, D.R., van Schrojenstein-Lantman, M.P., van der Horn, A.J., Denissen, I.F.C., Windows-Yule, C.R., de Jong, A.C. and Thornton, A.R. *MercuryDPM*: A Fast and Flexible Particle Solver Part A: Technical Advances. In: Li X., Feng Y., Mustoe G. (eds) *Proceedings of the 7th International Conference on Discrete Element Methods. DEM 2016.* Springer Proceedings in Physics, Springer, Singapore, Vol. 188, (2017).

[6] Luding, S. Introduction to discrete element methods. *European Journal of Environmental and Civil Engineering* (2008) **12**(7–8):785–826.

[7] Weinhart, T., Thornton, A. R., Luding, S. and Bokhove, O. From discrete particles to continuum fields near a boundary. *Granul. Matter* (2012) **14**(2):289–294.

[8] Tunuguntla, D.R., Thornton, A.R. and Weinhart, T. From discrete elements to continuum fields: Extension to bidisperse systems. *Comp. Part. Mech.* (2016) **3**:349–365.